

# Phenylpropanoids inhibit protofilament formation of *Escherichia coli* cell division protein FtsZ

Shanmugam Hemaiswarya, Rohini Soudaminikkutty,  
Mohana Lakshmi Narasumani and Mukesh Doble

Department of Biotechnology, Indian Institute of Technology Madras, Chennai 600 036, India

## Correspondence

Mukesh Doble

mukeshd@iitm.ac.in

The earliest step in cell division in bacteria is the assembly of FtsZ, an essential cell division protein, into a ring at the division site. FtsZ has GTPase activity and can assemble *in vitro* to form protein filaments. The present work involved the study of eight phenylpropanoids (cinnamic, *p*-coumaric, caffeic, chlorogenic, ferulic, 3,4-dimethoxycinnamic and 2,4,5-trimethoxycinnamic acids and eugenol) as inhibitors of *Escherichia coli* FtsZ. Phenylpropanoids make up the majority of our diet and act as antibacterial agents. Polymerization and GTPase inhibition assays showed that chlorogenic and caffeic acids were the most active amongst these (IC<sub>50</sub> of 70 and 106 μM, respectively). Circular dichroism studies indicated that chlorogenic acid perturbed the protein conformation and electron microscopy showed distorted filaments. *Bacillus subtilis* 168 cells treated with the phenylpropanoids were longer when compared to the control. The highest binding energy was observed between chlorogenic acid and the homology modelled *E. coli* FtsZ, which was consistent with the experimental results. A strong negative correlation was observed between binding energy and inhibition of the polymerization ability. 3D-Quantitative structure–activity relationship studies using GTPase activity indicated that the presence of more hydrophilic groups around the 3'- and 4'-carbon increased the activity. The effect of stress-induced formation of cell filamentation has to be understood before confirming the role of phenylpropanoids as FtsZ inhibitors.

Received 19 January 2011

Accepted 1 April 2011

## INTRODUCTION

Antimicrobial resistance is a global concern due to its increased prevalence. The major issues are the reduced susceptibility to currently available antimicrobial agents and shortage of newly approved compounds. A growing number of Gram-positive (*Staphylococcus aureus*, *Streptococcus pneumoniae*, etc.) and Gram-negative (*Pseudomonas aeruginosa*, *Klebsiella pneumoniae*, *Escherichia coli*, etc.) pathogens are responsible for infection in both the community and health-care settings (Furtado & Nicolau, 2010). Around 19–60 % of *Staphylococcus aureus* isolates from ocular infections have been shown to be resistant to macrolides, penicillin and fluoroquinolones (McDonald & Blondeau, 2010). The overall levels of antibiotic resistance can be dramatically decreased by focusing on the overuse of antibiotics, the pharmacokinetic and pharmacodynamic properties of different drug formulations, and use of proper hygiene

and protective barriers. There is also a need for the introduction of new antimicrobial agents with novel targets.

FtsZ is a bacterial cytoskeleton protein which assembles into a protofilament in a GTP-dependent manner. This forms a dynamic Z-ring at the mid-cell position. A study done in *E. coli* showed that 12 different proteins congregate at the Z-ring in a sequentially dependent pathway, causing assembly of the septal ring that guides the synthesis of the circumferential septum (Buddelmeijer & Beckwith, 2002; Bernhardt & de Boer, 2003; Romberg & Levin, 2003; Schmidt *et al.*, 2004). The septal ring constricts in concert with septal progression, culminating in complete disassembly as soon as it matures. Inhibition of this central protein perturbs the formation of the Z-ring and bacterial cytokinesis (Margolin, 2005). FtsZ has become an attractive target, due to its evolutionary distance from eukaryotic tubulin. There are many efforts to identify inhibitors of FtsZ that do not target eukaryotic tubulin. Interestingly, most of the agents that target tubulin/microtubule, including paclitaxel, vinblastine and colchicine, do not affect the dynamics of FtsZ assembly (Jaiswal *et al.*, 2007), indicating that the latter can be a selective antibacterial target.

PC190723, a synthetic compound (substituted benzamide and thiazolopyridine moieties linked with an ether bond), has been found to kill meticcillin-resistant *Staphylococcus*

**Abbreviations:** CD, circular dichroism; QSAR, quantitative structure–activity relationship.

Figures showing phenylpropanoid-induced filament formation in *B. subtilis* 168, the interaction of *E. coli* FtsZ with chlorogenic acid and a contribution plot of hydrophobic interactions are available as supplementary data with the online version of this paper.

*aureus*, many species of *Staphylococcus*, *Streptococcus* species, *Bacillus subtilis* and Gram-negative bacteria by targeting FtsZ (Haydon *et al.*, 2008). A range of compounds from natural sources including cinnamaldehyde (Domadia *et al.*, 2007), berberine (Domadia *et al.*, 2008), curcumin (Rai *et al.*, 2008), sanguinarine (Beuria *et al.*, 2005), ( $\pm$ )-dichamanetin and ( $\pm$ )-2''-hydroxy-5''-benzylisouvarinol-B (Urgaonkar *et al.*, 2005) have been reported to inhibit *E. coli* FtsZ. Small molecule inhibitors including 2-alkoxycarbonylaminopyridines (White *et al.*, 2002) and totarol (Jaiswal *et al.*, 2007) perturbed the functional properties of FtsZ from *Mycobacterium tuberculosis*.

The current study exploits the class of phenylpropanoids as FtsZ inhibitors. These compounds make up the majority of polyphenols consumed in our diet (Korkina, 2007). Members belonging to this class such as cinnamic acid, *p*-coumaric acid, caffeic acid, chlorogenic acid (Puupponen-Pimiä *et al.*, 2001), eugenol (Braga *et al.*, 2007; Hemaiswarya & Doble, 2009) and ferulic acid (Naz *et al.*, 2006; Hemaiswarya & Doble, 2010) acid have been shown to possess antimicrobial activity. The activity of these compounds toward bacteria is attributed to their membrane-damaging nature (Sung & Lee, 2010). They perturb the membrane lipid bilayers, causing the leakage of ions and other materials, as well as form pores and dissipate the electrical potential of the membrane (Sung & Lee, 2010).

## METHODS

**Materials.** GTP, 2,4,5-trimethoxycinnamic acid and eugenol were purchased from Sigma. Cinnamic, *p*-coumaric, caffeic and 3,4-dimethoxycinnamic acids, Luria-Bertani medium, Tris/HCl, KCl and MgCl<sub>2</sub> were purchased from Himedia. Chlorogenic acid, ferulic acid, MES and IPTG were purchased from SRL. All other chemicals were of analytical grade.

**Expression and purification of *E. coli* FtsZ.** *E. coli* FtsZ (*EcFtsZ*) was overexpressed and purified from the recombinant *E. coli* BL21 strain carrying pET11b (kindly provided by Professor H. P. Erickson, Duke University) as described previously (Lu *et al.*, 2001; Romberg *et al.*, 2001). The purity of the protein was analysed by 10% SDS-PAGE and its concentration was determined by the Bradford method (Bradford, 1976). The protein was aliquoted and stored at -80 °C. FtsZ was put through a cycle of calcium-aided assembly and disassembly to select the active and nonaggregated protein (Romberg *et al.*, 2001). All the following experiments were repeated in triplicate.

The inhibition of FtsZ GTPase activity was measured using a malachite green-phosphomolybdate assay (Akiyama *et al.*, 1996) with 6  $\mu$ M *EcFtsZ* in HEPES assembly buffer [50 mM 4-(2-hydroxyethyl)-1-piperazineethanesulfonic acid, pH 7.7; 5 mM magnesium acetate; 350 mM potassium acetate; 10 mM CaCl<sub>2</sub>] with 1 mM GTP. The compounds (in DMSO) were added to achieve a final concentration of 100  $\mu$ M and the DMSO concentration was maintained at 1%. FtsZ was preincubated with or without the phenylpropanoids for 5 min and the reactions were initiated by adding 1 mM GTP. Aliquots were withdrawn after 15 min of incubation and quenched with 20 mM EDTA. To 5  $\mu$ l reaction aliquots, 120  $\mu$ l malachite green solution and 30  $\mu$ l 34% (w/v) sodium citrate were added, the samples were incubated for 30 min at room temperature, and the A<sub>650</sub> was read

(UV-visible spectrometer V-550; Jasco). The per cent inhibition was calculated by comparing the rate of hydrolysis in the presence and absence of inhibitor.

**Inhibition of polymerization ability.** Inhibition of GTP-initiated *in vitro* polymerization of recombinant wild-type *E. coli* FtsZ by phenylpropanoids was assessed by a light-scattering assay (Mukherjee & Lutkenhaus, 1999). FtsZ (6  $\mu$ M) was polymerized in HEPES assembly buffer with 1 mM GTP in the presence of phenylpropanoids (0–250  $\mu$ M) and monitored in a Jasco fluorescence spectrometer with excitation and emission wavelengths set at 350 nm. Data were plotted as per cent inhibition of polymerization activity as a function of drug concentration. The curve was fitted to a four-parameter logistic function using SIGMAPLOT 10.0 (Systat Software) and the drug concentration required to inhibit the polymerization ability of FtsZ by 50% (IC<sub>50</sub>) was estimated.

**Visualization of bacterial morphology.** *B. subtilis* 168 was grown in the absence and presence of different concentrations of phenylpropanoids for 2 h in LB broth supplemented with 10 mM phenylpropanoids. The cells were fixed in 2.8% formaldehyde and 0.04% glutaraldehyde at 25 °C. The cells were collected, washed and resuspended in PBS (pH 7.4). Their morphology was examined under a differential interference contrast microscope (Nikon Eclipse 80i) at  $\times 40$  magnification. The cell length was measured using ImageJ 1.43u software (National Institutes of Health, USA).

**Electron microscopic analysis.** FtsZ at 6  $\mu$ M was polymerized in assembly buffer for 10 min. The protofilaments were treated with 100  $\mu$ M chlorogenic acid and samples were prepared for electron microscopy (Santra *et al.*, 2005). The images were collected using a JEOL 3010 transmission electron microscope.

**Analysis of changes in secondary structure.** FtsZ (6  $\mu$ M) was incubated without or with 100  $\mu$ M chlorogenic acid in 25 mM phosphate buffer (pH 6.5) for 15 min at 25 °C. The far-UV circular dichroism (CD) spectrum was monitored over a wavelength range of 190–250 nm using a Jasco J720 dichrograph equipped with a Peltier temperature controller and a 0.1 cm path length quartz cuvette. A mean of five scans was taken for each spectrum. K2D2, a method with an associated web server, was used to estimate protein secondary structure from CD spectra (Perez-Iratxeta & Andrade-Navarro, 2008).

**Molecular modelling.** The 3D structure of *E. coli* cell division protein FtsZ was constructed from the crystal structure of *Methanococcus jannaschii* FtsZ (PDB code: 1FSZ, 2.8 Å) (Domadia *et al.*, 2007; Löwe & Amos, 1998). Homology modelling was performed by using MODELLER version 9v7 (Šali & Blundell, 1993). The structures of the ligands were energy minimized and charges were added using ANTECHAMBER (AM1-BCC). The energy minimized ligands were docked to the modelled protein with AutoDock version 3.0 (Morris *et al.*, 1998). The grid maps for docking were prepared with Autogrid3. The active site was selected as the centre of the grid box and 56  $\times$  46  $\times$  52 points with grid spacing of 0.375 Å were calculated. A Lamarckian genetic algorithm was adopted to perform the molecular docking. The various genetic algorithm parameters were: a maximum of 250 000 energy evaluations; a maximum of 27 000 generations; mutation and crossover rates of 0.02 and 0.8, respectively; and 100 docking runs. The final docked conformations were clustered with a tolerance of 1.5 Å root-mean-square deviation. The best docked representation of the ligand was chosen based on the conformation with lowest binding free energy. Hydrogen bonding and hydrophobic interactions of the ligand with the protein were analysed using PyMOL software, v. 0.99 (DeLano, 2002).

**Development of a quantitative structure–activity relationship (QSAR).** A 3D-quantitative structure–activity relationship (QSAR)

was generated using V-Life Molecular Design Suite 3.0 (Vlife MDS). The set of eight molecules was divided into training and test sets (six in the training and two in the test sets). Here the activity is defined as  $\log [p/(100-p)]$ , where  $p$  is the percentage inhibition of GTP-initiated polymerization caused by the compounds at a concentration of 100  $\mu\text{M}$ . The structures of all the eight compounds were built with the software and their minimum energy conformations were estimated with the Monte Carlo conformational search algorithm with a root-mean-square gradient of 0.001 kcal mol<sup>-1</sup> and iteration limit of 10000 using Merck molecular force field 94. All the molecules were aligned on a common template. The steric, electrostatic and hydrophobic interaction energies at grid positions around these aligned molecules were estimated. Steric and electrostatic fields were computed at each grid point by calculating the interaction energy between the molecule and a probe molecule placed at each grid point considering Merck molecular force field charges (Halgren, 1996). The probe consisted of a methyl group of charge +1 with 10.0 kcal mol<sup>-1</sup> electrostatic and 30.0 kcal mol<sup>-1</sup> steric cut-off. A value of 1.0 is assigned for distance-dependent dielectric constant (Cramer *et al.*, 1988). Several regression relations between these descriptors and the activity were generated using molecular field analysis coupled with partial least-squares. The best model was selected on the basis of various statistical parameters, namely squared correlation coefficient ( $r^2$ ), cross validated square correlation coefficient ( $q^2$ ), predicted  $r^2$  and sequential Fisher test (F).

## RESULTS

### Phenylpropanoids inhibit GTPase activity

The dynamics of FtsZ assembly is regulated by the hydrolysis of GTP (Mukherjee *et al.*, 2001). Most of the phenylpropanoids reduced the GTPase activity of *EcFtsZ* at a concentration of 100  $\mu\text{M}$  (Fig. 1). For example, 100  $\mu\text{M}$  chlorogenic and ferulic acids inhibited the GTPase activity by 46 and 34 %, respectively. Caffeic and *p*-coumaric acid reduced GTPase activity by 23 and 29 %, respectively, when compared to the control ( $P < 0.001$ ). The rest of the phenylpropanoids exhibited lesser activity (in the range of 15–20 %) than the above compounds. GTPase activity is

required for the dynamics of FtsZ assembly and therefore inhibition of this activity will perturb the formation of protofilament.

### Inhibition of FtsZ assembly by phenylpropanoids

The kinetics of assembly of FtsZ is measured semiquantitatively *in vitro* in terms of an increase in the light scattering at 350 nm (Mukherjee & Lutkenhaus, 1999). Most of the phenylpropanoids inhibited FtsZ assembly in a dose-dependent manner (Fig. 2). Chlorogenic acid inhibited GTP-initiated FtsZ polymerization by 77, 57, 45 and 27 % at 200, 100, 50 and 25  $\mu\text{M}$  concentrations, respectively, after 15 min and the IC<sub>50</sub> was estimated to be approximately 70  $\mu\text{M}$ . Table 1 lists the effect of phenylpropanoids on the polymerization of *EcFtsZ*. Caffeic, *p*-coumaric and 2,4,5-trimethoxycinnamic acids inhibited FtsZ assembly with IC<sub>50</sub> values between 100 and 200  $\mu\text{M}$ . The IC<sub>50</sub> values for eugenol and ferulic and 3,4-dimethoxycinnamic acids were more than 250  $\mu\text{M}$ . The effect of chlorogenic acid on the assembly of FtsZ was visualized by transmission electron microscopy (Fig. 3). The control showed thick bundles of FtsZ polymers. A high concentration (100  $\mu\text{M}$ ) of chlorogenic acid under the polymerization conditions induced aggregation of FtsZ monomers and distorted protofilaments.

### Effect of phenylpropanoids on the morphology of *B. subtilis* 168

Most of the phenylpropanoids induced filamentation in *B. subtilis* 168 cells. The mean length of this micro-organism was  $5.4 \pm 1.3 \mu\text{m}$  and it increased by 3.2-fold to  $13.7 \pm 6.2 \mu\text{m}$  after 2 h of incubation with 100 mM chlorogenic acid. In the presence of 100 mM cinnamic, *p*-coumaric, caffeic, ferulic and 2,4,5-trimethoxycinnamic acids, the mean length of *B. subtilis* 168 cells increased by one- to twofold

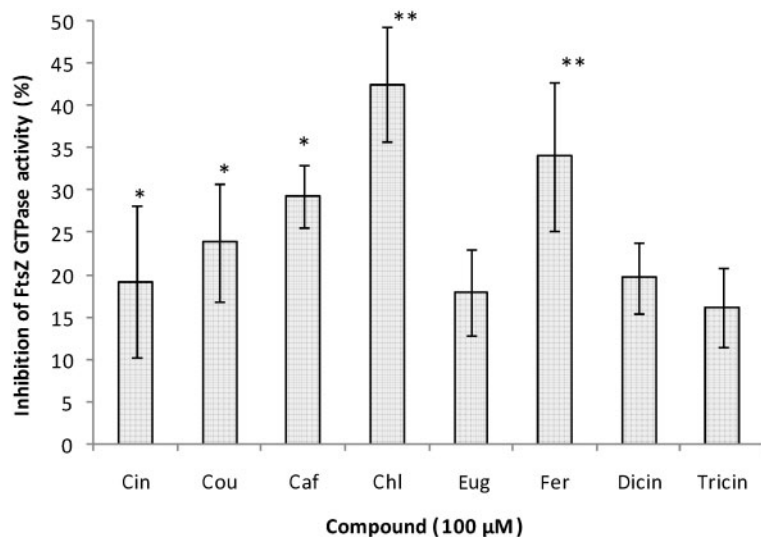


**Fig. 1.** Effect of phenylpropanoids on the GTPase activity (15 min) of *E. coli* FtsZ. \*\* $P < 0.001$ ; \* $P < 0.05$ .

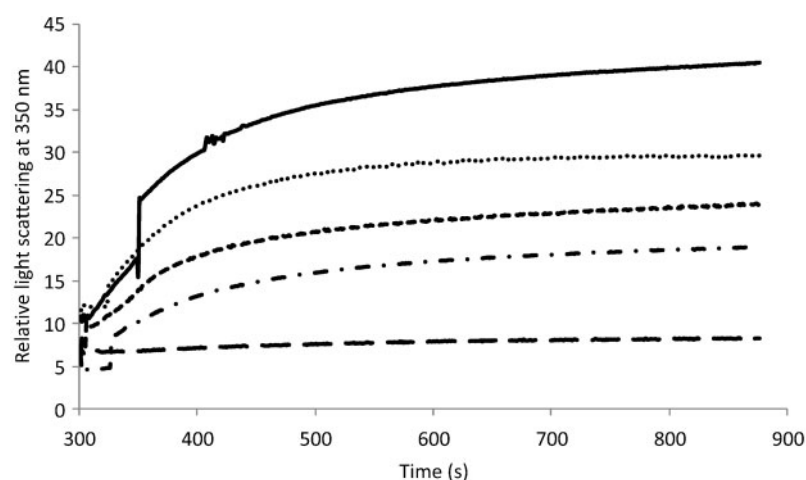


**Fig. 2.** FtsZ polymerized in the absence (—) and presence of 25  $\mu\text{M}$  (…), 50  $\mu\text{M}$  (---), 100  $\mu\text{M}$  (-·-) and 200  $\mu\text{M}$  (— —) chlorogenic acid.

(Table 2). Eugenol and 3,4-dimethoxycinnamic acid did not increase the mean length.

Most of the phenylpropanoid-treated cells were strikingly longer than the control (vehicle-treated) cells. In the case of the control, 44% of the cells had a mean length in the range of 3–5  $\mu\text{m}$  (Supplementary Fig. S1 in JMM Online). More than 40% of cells treated with caffeic, chlorogenic, ferulic and 2,4,5-trimethoxycinnamic acids had a length >11  $\mu\text{m}$  and more than 30% of cells were >11  $\mu\text{m}$  when treated with cinnamic and *p*-coumaric acid. These results indicate that phenylpropanoids inhibit bacterial proliferation by inhibiting cytokinesis and thereby increase the cell length.

### Effect of chlorogenic acid on the secondary structure of FtsZ

The effect of 100  $\mu\text{M}$  chlorogenic acid on the secondary structure of FtsZ was determined with far-UV CD spectra. Analysis of these spectra using deconvolution software, K2D2 (Perez-Iratxeta & Andrade-Navarro, 2008), indicated that the secondary structure of FtsZ contained  $39.37\% \pm 0.8$  and  $11.52\% \pm 0.6$  of  $\alpha$ -helix and  $\beta$ -strand, respectively. Chlorogenic acid perturbed the secondary structure of FtsZ (Fig. 4) by reducing the helical content by 23.8% (from 39.37% to  $29.97 \pm 0.5\%$ ) and increasing the  $\beta$ -strand content by 18.6% (from 11.52% to 13.66%). The troughs at 208 and 222 nm are characteristic of the high content of  $\alpha$ -helix, which is disrupted due to chlorogenic acid treatment. These observed changes were statistically significant ( $P < 0.001$ ).

### Modelling

The amino acids in the active sites of *E. coli* cell division protein FtsZ are Asn207, Asp209, Asp212 and Arg214, which are equivalent to those found in *M. jannaschii* (namely Asn233, Asp235, Asp238 and Lys240). These two proteins share a sequence similarity of 46.3%. Hence the structure of *M. jannaschii* FtsZ (PDB code: 1FSZ) can be

considered a valid template for building the homology model. Docking of various compounds to the protein showed that chlorogenic acid had the highest binding energy when compared to the rest (Table 3). Hydroxyl groups in chlorogenic acid formed hydrogen bonds with Ala11, Gly36, Asn207, Val208, Asp209 and Phe210 (Supplementary Fig. S2). The complex was further stabilized by the hydrophobic interaction with Pro203 and polar contact with Asn207. The latter is located in the T7 loop of the protein and it has been suggested to be part of the active site region (Scheffers *et al.*, 2002). The order of increase in binding energy was chlorogenic acid > ferulic acid > caffeic acid > *p*-coumaric acid > cinnamic acid > 3,4-dimethoxycinnamic acid > eugenol > 2,4,5-trimethoxycinnamic acid. Almost all the phenylpropanoids interacted with at least one residue in the T7 loop.

### QSAR analysis

The inhibition of GTPase activity of FtsZ by phenylpropanoids at a concentration of 100  $\mu\text{M}$  was used to generate the 3D-QSAR. The percentage inhibition reported in Table 1 was converted to activity, defined as  $\log [p/(100-p)]$ : activity =  $-(1.8) H_{214} + 0.01$ ,  $r^2 = 0.7$ ,  $q^2 = 0.6$ ,  $F = 10.6$ ,  $\text{pred}_r^2 = 0.6$ .

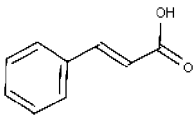
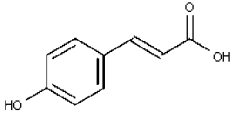
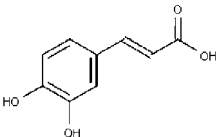
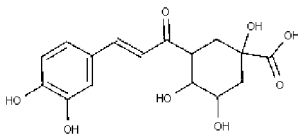
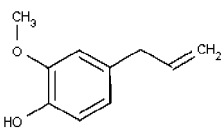
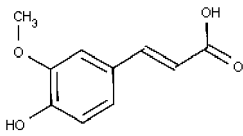
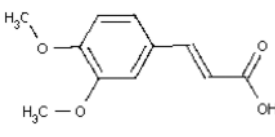
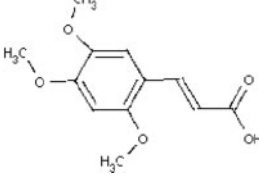
$H_{214}$  is a hydrophobic descriptor at the spatial grid point 214 (Supplementary Fig. S3). A hydrophobic descriptor with negative coefficient ( $H_{214}$ ) around the third and fourth position of the benzene ring indicates that hydrophilic groups are preferred for enhanced activity. All the statistical parameters estimated were reasonably good indicating the quality of the QSAR developed.

### DISCUSSION

Phenylpropanoids belong to the largest group of secondary metabolites produced by plants, mainly in response to biotic or abiotic stresses such as infections, wounding, UV irradiation, pollutants and other hostile environmental

**Table 1.** Effect of phenylpropanoids on *in vitro* assembly of FtsZ

The polymerization of GTP-induced FtsZ was monitored as a function of light scattering for 15 min.

Compound	Structure	IC <sub>50</sub> (μM) ± SEM	% inhibition (100 μM)
Cinnamic acid		238.91 ± 7.1	24.17 ± 4.9
<i>p</i> -Coumaric acid		189.53 ± 3.7	26.83 ± 3.1
Caffeic acid		105.96 ± 6.3	45.76 ± 12.9
Chlorogenic acid		69.55 ± 3.6	57.04 ± 5.6
Eugenol		>250	15.89 ± 2.6
Ferulic acid		>250	19.1 ± 2.3
3,4-Dimethoxycinnamic acid		>250	12.7 ± 3.5
2,4,5-Trimethoxycinnamic acid		148.59 ± 4.3	29.8 ± 5.2

conditions (Korkina, 2007). The current study shows that they inhibit FtsZ assembly, thereby perturbing the formation of the Z-ring, and finally inhibiting the process of cell division. This inhibition was confirmed by the reduction in light scattering of polymerized FtsZ. They also inhibited GTPase activity of FtsZ, indicating their ability to depolymerize preformed FtsZ polymers. Structures similar to the phenylpropanoids such as curcumin (a dimer with a phenylpropanoid group) and cinnamaldehyde have been reported to inhibit *E. coli* FtsZ (Domadia *et al.*, 2007; Rai *et al.*, 2008).

In the current list of eight phenylpropanoids, chlorogenic (IC<sub>50</sub>=70 μM) and caffeic acids were good inhibitors of FtsZ. Chlorogenic acid is an ester of caffeic acid and quinic acid. The decrease in the polymerization and bundling of FtsZ may be due to the conformational changes induced by chlorogenic acid in the FtsZ monomer. FtsZ may not be the primary target for chlorogenic acid. Antifungal studies against *Candida albicans* indicated that it disrupts the structure of the cell membrane (Sung & Lee, 2010). Caffeic acid also inhibited FtsZ assembly, though at a slightly

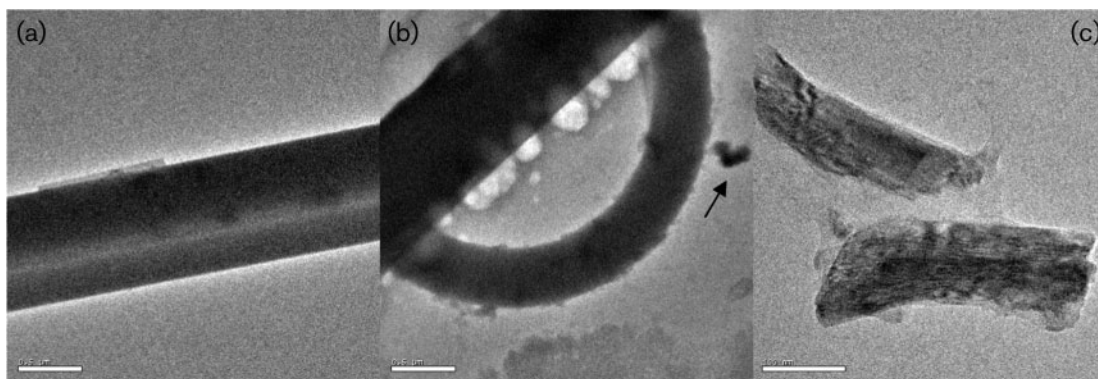


**Fig. 3.** Inhibitory effect of chlorogenic acid on preformed FtsZ wild-type protofilaments as viewed by electron microscopy. (a) Control; (b, c) treated with 100  $\mu\text{M}$  chlorogenic acid. The arrow indicates aggregates formed. (c) Distorted protofilaments. Bars, 500  $\mu\text{m}$  (a, b) and 100  $\mu\text{m}$  (c).

higher  $\text{IC}_{50}$  (at 106  $\mu\text{M}$ ), followed by *p*-coumaric acid. Caffeic and *p*-coumaric acid were reported by other researchers to cause 44 and 59% membrane damage, respectively, on a Gram-positive bacterium, *Oenococcus oeni* (Campos *et al.*, 2009). This suggests that these phenylpropanoids act not only through targeting FtsZ but also through membrane perturbation. Ferulic acid at 100  $\mu\text{M}$  has high GTPase inhibition activity (~26%). Though the inhibition of polymerization ability of FtsZ by ferulic acid was poor ( $\text{IC}_{50} > 250 \mu\text{M}$ ), there was a significant increase in the cell length of *B. subtilis* 168. Also ferulic acid at 10 mM has been shown to possess a very low membrane-damaging activity (less than 5%) against Gram-negative bacteria (Hemaiswarya & Doble, 2010). The phenylpropanoids being small molecules have multiple targets. Eugenol was found to be less active against the inhibition of GTPase and polymerization activities. There was no increase in the cell size of *B. subtilis* 168 treated with eugenol when compared with that of the control. Eugenol is reported to primarily act by disrupting the cytoplasmic membrane (Hemaiswarya & Doble, 2009; Gill & Holley, 2006). Cinnamic, *p*-coumaric, caffeic, chlorogenic and 2,4,

5-trimethoxycinnamic acids and eugenol have been shown to damage the bacterial membrane of Gram-negative and Gram-positive bacteria (Hemaiswarya & Doble, 2009; Gill & Holley, 2006). Previous studies (Rastogi *et al.*, 2008) have shown the potential of a few phytochemicals to inhibit FtsZ assembly under *in vitro* conditions. *trans*-Cinnamic acid was found to be the most potent inhibitor; however, naringenin, eugenol and 4-formyl cinnamic acid did not show considerable inhibition of FtsZ polymerization. Our results also substantiate the above study, where cinnamic acid inhibited FtsZ assembly and eugenol was inactive.

Docking studies indicated that all the phenylpropanoids interacted with at least one of the residues in the T7 loop of FtsZ. Structural analysis of the organization of FtsZ subunits in the polymers, in wild-types as well in mutants, indicates the important role of the T7-loop region ('tubulin-loop' no. 7) (Nogales *et al.*, 1998) of FtsZ in the self-association of the monomers. The T7 loop is highly conserved among FtsZ proteins from different species. Modelling of the crystal structure of *M. jannaschii* FtsZ1 onto electron microscopy images of protofilaments of FtsZ1 has shown that the active site for GTP hydrolysis may be shared by two FtsZ subunits, with the GTP-binding domain located on one monomer and modulation of hydrolysis by the T7 loop of the other domain (Löwe & Amos, 1999). FtsZ proteins contain a conserved sequence that is homologous to the Walker B motif present in a large number of ATP-binding proteins (Walker *et al.*, 1982; Burke *et al.*, 1990). The *E. coli* FtsZ residues 208–212 (VDFAD) conform to the motif '(hydrophobic, aliphatic)-X-aromatic-X-acidic' (part of the Walker B sequence), which has been implicated as the  $\text{Mg}^{2+}$ -binding site consensus sequence in adenylate kinase, ATPases and myosins (Walker *et al.*, 1982; Burke *et al.*, 1990; Farr & Sternlicht, 1992). Interaction of phenylpropanoids with these residues would probably result in the perturbation of the conformation of the T7 loop, which is involved in the GTPase activity of the FtsZ (Scheffers *et al.*, 2002). Our

**Table 2.** Mean length of *B. subtilis* 168 cells in the presence (100  $\mu\text{M}$ ) and absence of phenylpropanoids

Treatment	Mean length ( $\mu\text{m}$ )
Control (without treatment)	5.4 $\pm$ 1.3
Cinnamic acid	12.7 $\pm$ 8.9*
<i>p</i> -Coumaric acid	11.9 $\pm$ 8.4*
Caffeic acid	11.9 $\pm$ 8.2*
Chlorogenic acid	13.67 $\pm$ 6.2*
Eugenol	5.24 $\pm$ 3.9
Ferulic acid	10.9 $\pm$ 9.3*
3,4-Dimethoxycinnamic acid	6.9 $\pm$ 4.4*
2,4,5-Trimethoxycinnamic acid	12.06 $\pm$ 8.9*

\* $P < 0.05$ .

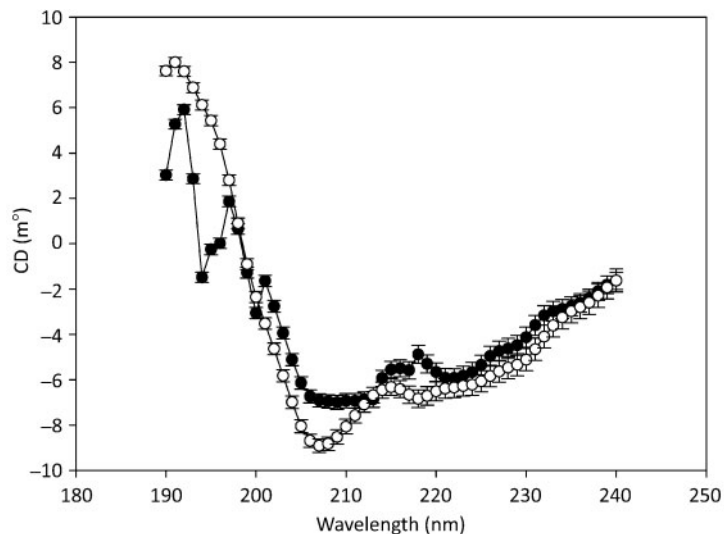


**Fig. 4.** CD spectra of FtsZ alone (○) and treated with 100  $\mu$ M chlorogenic acid (●).

experiments have shown that phenylpropanoids inhibit the GTPase activity of FtsZ, further validating the above proposition. The crystal structure of the SOS-inducible cell division inhibitor Sula in complex with FtsZ from *Pseudomonas aeruginosa* revealed that Sula binds to the T7-loop surface of FtsZ (Cordell *et al.*, 2003). These compounds may bind to the T7 loop in one FtsZ monomer, inducing such conformational changes that it fails to make optimum contact with the GTP binding

T1–T6 loop in the neighbouring monomer and thereby inhibiting FtsZ polymerization.

The 3D-QSAR indicates the need for hydrophilic groups at the third and fourth carbon of the benzene ring for high activity. Chlorogenic and caffeic acid possess a hydroxyl group, making them more hydrophilic than the other compounds, which have methoxy substituents, hence they exhibit highest activity. The presence of more hydroxyl groups favours hydrogen bonds with the amino acid side chains in the active site. Molecular docking studies also indicate that chlorogenic acid interacts with FtsZ through hydrogen bonds.

The present work suggests that phenylpropanoids could be considered as a new source for the development of antibacterial drugs. The study involves inhibition under *in vitro* conditions, and their *in vivo* performance has to be speculated. Chlorogenic and caffeic acids could be the lead structures for the design of more stable and potent anti-FtsZ agents as well as a vital tool for understanding the regulatory role of FtsZ in cell division. Cell wall damage, which remains a likely mode of action, is known to induce the SOS response and cell filamentation. Two additional experiments are needed to support the above claims, namely: (i) induction of cell filamentation in an SOS mutant of an *E. coli* strain, which will control again many stress related pathways to filamentation; and (ii) over- or underexpression of the gene encoding FtsZ, leading to resistance of sensitivity to the compounds, which will help to prove whether the compounds act by FtsZ inhibition or not. Also, it would be worth trying to visualize the Z-rings by fluorescence microscopy and see the effect of these compounds on their formation.

**Table 3.** Docking results with modelled FtsZ (*E. coli*)

Ligand	Binding energy	H-bonds	Distance (Å)
Cinnamic acid	−5.68	Met206	2.158
		Thr296	1.898
<i>p</i> -Coumaric acid	−5.72	Met206	2.219
		Thr296	1.866
Caffeic acid	−6.17	Met206	2.212
		Thr296	1.849
Chlorogenic acid	−8.36	Ala11	1.777
		Gly36	1.949
		Asn207	2.12
		Val208	2.217
		Asp209	2.138
Eugenol	−5.26	Phe210	2.168
		Thr201	2.228
Ferulic acid	−6.33	Ala11	2.194
		Gly204	2.107
		Met206	1.783
		Val208	2.236
3,4-Dimethoxycinnamic acid	−5.46	Ala11	1.834
		Val208	1.691
2,4,5-Trimethoxycinnamic acid	−5.18	Ala11	2.079
		Val208	1.689

## ACKNOWLEDGEMENTS

The authors thank Professor H. P. Erickson (Duke University) for providing the *E. coli* BL21 strain carrying pET11b.

## REFERENCES

- Akiyama, Y., Kihara, A., Tokuda, H. & Ito, K. (1996). FtsH (HflB) is an ATP-dependent protease selectively acting on SecY and some other membrane proteins. *J Biol Chem* **271**, 31196–31201.
- Bernhardt, T. G. & de Boer, P. A. (2003). The *Escherichia coli* amidase AmiC is a periplasmic septal ring component exported via the twin-arginine transport pathway. *Mol Microbiol* **48**, 1171–1182.
- Beuria, T. K., Santra, M. K. & Panda, D. (2005). Sanguinarine blocks cytokinesis in bacteria by inhibiting FtsZ assembly and bundling. *Biochemistry* **44**, 16584–16593.
- Bradford, M. M. (1976). A rapid and sensitive method for the quantitation of microgram quantities of protein utilizing the principle of protein-dye binding. *Anal Biochem* **72**, 248–254.
- Braga, P. C., Sasso, M. D., Culici, M. & Alfieri, M. (2007). Eugenol and thymol, alone or in combination, induce morphological alterations in the envelope of *Candida albicans*. *Fitoterapia* **78**, 396–400.
- Buddelmeijer, N. & Beckwith, J. (2002). Assembly of cell division proteins at the *E. coli* cell center. *Curr Opin Microbiol* **5**, 553–557.
- Burke, M., Rajasekharan, K. N., Maruta, S. & Ikebe, M. (1990). A second consensus sequence of ATP-requiring proteins resides in the 21-kDa C-terminal segment of myosin subfragment 1. *FEBS Lett* **262**, 185–188.
- Campos, F. M., Couto, J. A., Figueiredo, A. R., Tóth, I. V., Rangel, A. O. S. S. & Hogg, T. A. (2009). Cell membrane damage induced by phenolic acids on wine lactic acid bacteria. *Int J Food Microbiol* **135**, 144–151.
- Cordell, S. C., Robinson, E. J. H. & Lowe, J. (2003). Crystal structure of the SOS cell division inhibitor SulaA and in complex with FtsZ. *Proc Natl Acad Sci U S A* **100**, 7889–7894.
- Cramer, R. D., Patterson, D. E. & Bunce, J. D. (1988). Comparative molecular field analysis (CoMFA). 1. Effect of shape on binding of steroids to carrier proteins. *J Am Chem Soc* **110**, 5959–5967.
- DeLano, W. L. (2002). *The PyMOL Molecular Graphics System*. Palo Alto, CA: DeLano Scientific.
- Domadia, P., Swarup, S., Bhunia, A., Sivaraman, J. & Dasgupta, D. (2007). Inhibition of bacterial cell division protein FtsZ by cinnamaldehyde. *Biochem Pharmacol* **74**, 831–840.
- Domadia, P. N., Bhunia, A., Sivaraman, J., Swarup, S. & Dasgupta, D. (2008). Berberine targets assembly of *Escherichia coli* cell division protein FtsZ. *Biochemistry* **47**, 3225–3234.
- Farr, G. W. & Sternlicht, H. (1992). Site-directed mutagenesis of the GTP-binding domain of  $\beta$ -tubulin. *J Mol Biol* **227**, 307–321.
- Furtado, G. H. & Nicolau, D. P. (2010). Overview perspective of bacterial resistance. *Expert Opin Ther Pat* **20**, 1273–1276.
- Gill, A. O. & Holley, R. A. (2006). Disruption of *Escherichia coli*, *Listeria monocytogenes* and *Lactobacillus sakei* cellular membranes by plant oil aromatics. *Int J Food Microbiol* **108**, 1–9.
- Halgren, T. A. (1996). Merck molecular force field. III. Molecular geometries and vibrational frequencies. *J Comput Chem* **17**, 553–586.
- Haydon, D. J., Stokes, N. R., Ure, R., Galbraith, G., Bennett, J. M., Brown, D. R., Baker, P. J., Barynin, V. V., Rice, D. W. & other authors (2008). An inhibitor of FtsZ with potent and selective anti-staphylococcal activity. *Science* **321**, 1673–1675.
- Hemaiswarya, S. & Doble, M. (2009). Synergistic interaction of eugenol with antibiotics against Gram negative bacteria. *Phytomedicine* **16**, 997–1005.
- Hemaiswarya, S. & Doble, M. (2010). Synergistic interaction of phenylpropanoids with antibiotics against bacteria. *J Med Microbiol* **59**, 1469–1476.
- Jaiswal, R., Beuria, T. K., Mohan, R., Mahajan, S. K. & Panda, D. (2007). Tatarol inhibits bacterial cytokinesis by perturbing the assembly dynamics of FtsZ. *Biochemistry* **46**, 4211–4220.
- Korkina, L. G. (2007). Phenylpropanoids as naturally occurring antioxidants: from plant defense to human health. *Cell Mol Biol (Noisy-le-grand)* **53**, 15–25.
- Löwe, J. & Amos, L. A. (1998). Crystal structure of the bacterial cell-division protein FtsZ. *Nature* **391**, 203–206.
- Löwe, J. & Amos, L. A. (1999). Tubulin-like protofilaments in Ca<sup>2+</sup>-induced FtsZ sheets. *EMBO J* **18**, 2364–2371.
- Lu, C., Stricker, J. & Erickson, H. P. (2001). Site-specific mutations of FtsZ – effects on GTPase and *in vitro* assembly. *BMC Microbiol* **1**, 7.
- Margolin, W. (2005). FtsZ and the division of prokaryotic cells and organelles. *Nat Rev Mol Cell Biol* **6**, 862–871.
- McDonald, M. & Blondeau, J. M. (2010). Emerging antibiotic resistance in ocular infections and the role of fluoroquinolones. *J Cataract Refract Surg* **36**, 1588–1598.
- Morris, G. M., Goodsell, D. S., Halliday, R. S., Huey, R., Hart, W. E., Belew, R. K. & Olson, A. J. (1998). Automated docking using a Lamarckian genetic algorithm and empirical binding free energy function. *J Comput Chem* **19**, 1639–1662.
- Mukherjee, A. & Lutkenhaus, J. (1999). Analysis of FtsZ assembly by light scattering and determination of the role of divalent metal cations. *J Bacteriol* **181**, 823–832.
- Mukherjee, A., Saez, C. & Lutkenhaus, J. (2001). Assembly of an FtsZ mutant deficient in GTPase activity has implications for FtsZ assembly and the role of the Z ring in cell division. *J Bacteriol* **183**, 7190–7197.
- Naz, S., Ahmad, S., Ajaz Rasool, S., Asad Sayeed, S. & Siddiqi, R. (2006). Antibacterial activity directed isolation of compounds from *Onosma hispidum*. *Microbiol Res* **161**, 43–48.
- Nogales, E., Downing, K. H., Amos, L. A. & Löwe, J. (1998). Tubulin and FtsZ form a distinct family of GTPases. *Nat Struct Biol* **5**, 451–458.
- Perez-Iratxeta, C. & Andrade-Navarro, M. A. (2008). K2D2: estimation of protein secondary structure from circular dichroism spectra. *BMC Struct Biol* **8**, 25.
- Puupponen-Pimiä, R., Nohynek, L., Meier, C., Kähkönen, M., Heinonen, M., Hopia, A. & Oksman-Caldentey, K.-M. (2001). Antimicrobial properties of phenolic compounds from berries. *J Appl Microbiol* **90**, 494–507.
- Rai, D., Singh, J. K., Roy, N. & Panda, D. (2008). Curcumin inhibits FtsZ assembly: an attractive mechanism for its antibacterial activity. *Biochem J* **410**, 147–155.
- Rastogi, N., Domadia, P., Shetty, S. & Dasgupta, D. (2008). Screening of natural phenolic compounds for potential to inhibit bacterial cell division protein FtsZ. *Indian J Exp Biol* **46**, 783–787.
- Romberg, L. & Levin, P. A. (2003). Assembly dynamics of the bacterial cell division protein FtsZ: poised at the edge of stability. *Annu Rev Microbiol* **57**, 125–154.
- Romberg, L., Simon, M. & Erickson, H. P. (2001). Polymerization of FtsZ, a bacterial homolog of tubulin: is assembly cooperative? *J Biol Chem* **276**, 11743–11753.
- Šali, A. & Blundell, T. L. (1993). Comparative protein modelling by satisfaction of spatial restraints. *J Mol Biol* **234**, 779–815.
- Santra, M. K., Dasgupta, D. & Panda, D. (2005). Deuterium oxide promotes assembly and bundling of FtsZ protofilaments. *Proteins* **61**, 1101–1110.
- Scheffers, D.-J., de Wit, J. G., den Blaauwen, T. & Driessen, A. J. M. (2002). GTP hydrolysis of cell division protein FtsZ: evidence that the active site is formed by the association of monomers. *Biochemistry* **41**, 521–529.

**Schmidt, K. L., Peterson, N. D., Kustus, R. J., Wissel, M. C., Graham, B., Phillips, G. J. & Weiss, D. S. (2004).** A predicted ABC transporter, FtsEX, is needed for cell division in *Escherichia coli*. *J Bacteriol* **186**, 785–793.

**Sung, W. S. & Lee, D. G. (2010).** Antifungal action of chlorogenic acid against pathogenic fungi, mediated by membrane disruption. *Pure Appl Chem* **82**, 219–226.

**Urgaonkar, S., La Pierre, H. S., Meir, I., Lund, H., RayChaudhuri, D. & Shaw, J. T. (2005).** Synthesis of antimicrobial natural products

targeting FtsZ: ( $\pm$ )-dichamanetin and ( $\pm$ )-2'''-hydroxy-5''-benzylisouvarinol-B. *Org Lett* **7**, 5609–5612.

**Walker, J. E., Saraste, M., Runswick, M. J. & Gay, N. J. (1982).** Distantly related sequences in the alpha- and beta-subunits of ATP synthase, myosin, kinases and other ATP-requiring enzymes and a common nucleotide binding fold. *EMBO J* **1**, 945–951.

**White, E. L., Suling, W. J., Ross, L. J., Seitz, L. E. & Reynolds, R. C. (2002).** 2-Alkoxy-carbonylaminopyridines: inhibitors of *Mycobacterium tuberculosis* FtsZ. *J Antimicrob Chemother* **50**, 111–114.